# Self-phase modulation and frequency generation with few-cycle optical pulses in nonlinear dispersive media

Arkadiy A. Drozdov,[1,2] Sergey A. Kozlov,[1,*] Andrey A. Sukhorukov,[2] and Yuri S. Kivshar[2]
[1]*National Research University of Information Technologies, Mechanics and Optics, Saint Petersburg 197101, Russia*
[2]*Nonlinear Physics Centre, Research School of Physics and Engineering, Australian National University, Canberra, Australian Capital Territory 0200, Australia*
(Received 5 March 2012; published 19 November 2012)

We analyze nonlinear effects associated with the spatiotemporal propagation of few-cycle optical pulses in nonlinear dispersive media, including nonlinearity-induced self-phase modulation, generation of higher harmonics, and the effects of diffraction. First, we discuss the nonlinear equations governing the spatiotemporal propagation of short pulses in dispersive and diffractive nonlinear media and demonstrate a link between the field equation and the cubic nonlinear Schrödinger equation employed for describing the evolution of the pulse envelope. Then, for several different regimes of competitive scales, we study the self-action effects of few-cycle pulses and describe, both analytically and numerically, the pulse self-modulation and self-focusing, including the transformation of the spectral density and harmonic generation in the cases of weak and strong dispersion. Finally, we analyze the effect of the beam diffraction on self-action of the Gaussian few-cycle pulses.

DOI: 10.1103/PhysRevA.86.053822 PACS number(s): 42.65.Ky, 42.65.Jx, 42.65.Re

## I. INTRODUCTION

Recent progress in the advanced methods of ultrafast nonlinear optics led to the generation and control of very short pulses with durations of a few optical cycles (see, e.g., the review paper [1] and references therein). The study of the propagation of intense short optical pulses has opened a door to the analysis of novel effects of the so-called extreme nonlinear optics [2,3] and attosecond physics [4] allowing one to control and measure few-cycle light pulses and employ them for various applications in the problems of light-matter interaction. Advances with experimental studies of nonlinear effects with few cycles toward subcycle field structures motivate the expanding theoretical studies of related problems. Since the conventional slowly varying envelope approximation is not valid for describing the evolution of the electric-field profiles of ultrashort pulses containing only a few field oscillations, various authors derived the generalized nonlinear equations for describing the evolution of the pulse envelope [5–10] and also applied the generalized Schrödinger equation to study few-cycle optical solitons [11,12].

When the pulse becomes shorter, the nonlinearity leads to the pulse steepening effects, which are not well described by the approach employing the pulse envelope. To analyze the problem of the competition between spatial and temporal scales in the problem of the spatiotemporal self-phase modulation of few-cycle optical pulses, we should analyze the full equations, not reducing them to the wave dynamics of the envelope. This idea motivated the development of equations directly for the electric field of an optical pulse (see a recent review in Ref. [13]). The so-called short-pulse equations can be expressed in a rather simple form in the case of unidirectional propagation [14–23], and the models taking into account the beam diffraction can describe complex spatiotemporal dynamics [24–32]. The field equations have been used, in particular, to study self-focusing and spatiotemporal collapse dynamics of optical pulses [27–29,31–33]. However, detailed investigation of self-phase modulation phenomena and harmonic generation of few-cycle pulses in the framework of the field equations has not been performed.

Here, we summarize the results of our systematic analytical and numerical analysis of optical harmonic generation in the process of few-cycle optical pulse self-action in cubic nonlinear dispersive media. We discuss several different regimes of competition between spatial and temporal scaling parameters and also the relation between the field equations and the conventional equations for the pulse envelopes. In particular, we study numerically the self-action of few-cycle pulses such as self-modulation and self-focusing and analyze the transformation of the spectral density and harmonic generation in the cases of weak and strong dispersion. Finally, we analyze the effect of the beam diffraction on the self-action and harmonic generation by few-cycle pulses.

The paper is organized as follows. Section II is devoted to the discussion of the model that is a reduced model for the unidirectional paraxial spatiotemporal evolution of optical pulses in a nonlinear medium; this model was derived earlier [24,25]. Here we describe the reduction of this model to the equation for the wave envelope as well as discuss the generalization of this model to describe the generation of the third harmonics. In Sec. III we study the pulse propagation in media with weak dispersion and diffraction, when many results can be obtained analytically, by means of the perturbation theory. This includes also the analysis of the third-harmonic generation and the dependence of this process on the pulse duration. Section IV is devoted to the analysis of dispersion on the pulse self-action, whereas Sec. V summarizes our results on the effect of the diffraction. Finally, Sec. VI concludes the paper.

## II. EQUATIONS FOR THE FIELD DYNAMICS IN NONLINEAR MEDIA

We now formulate the model equation to simulate the evolution of a linearly polarized optical beam in an isotropic

*kozlov@mail.ifmo.ru

 

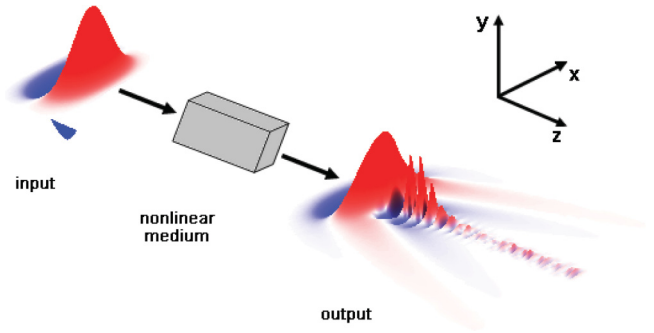


FIG. 1. (Color online) Example of the propagation of a single-cycle paraxial beam in a nonlinear medium. The beam undergoes strong temporal reshaping and diffracting in space.

dielectric medium with instant Kerr-type nonlinear response, accounting for spatiotemporal effects, as schematically illustrated in Fig. 1. We consider the unidirectional paraxial propagation corresponding to a beam width much larger than the optical wavelength, and assume that the wavelength spectrum is within the region of the normal group-velocity dispersion. Under such conditions, the following equation has been derived for the electric field of an optical wave $E(x,y,z,t)$ [25]:

$$\frac{\partial E}{\partial z} + K_0 E + \frac{N_0}{c}\frac{\partial E}{\partial t} - K_1 \frac{\partial^2 E}{\partial t^2} - a\frac{\partial^3 E}{\partial t^3} + gE^2\frac{\partial E}{\partial t} = \frac{c}{2N_0}\Delta_\perp \int_{-\infty}^{t} E dt', \tag{1}$$

where $z$ is the distance along the propagation direction, $\Delta_\perp = \partial^2/\partial x^2 + \partial^2/\partial y^2$ is the transverse Laplace operator, $t$ is time, and $c$ is the speed of light in a vacuum. It is straightforward to determine the frequency dispersion of the linear refractive index associated with Eq. (1) by substituting a plane-wave solution $E(z,x,y,t) = (1/2)\exp[ik(\omega)z - i\omega_0 t] + \text{c.c.}$ (where c.c. stands for a complex conjugate) and neglecting nonlinear terms. We obtain

$$k(\omega) = k_r(\omega) + ik_i(\omega) = (N_0\omega c^{-1} + a\omega^3) + i(K_0 + K_1\omega^2), \tag{2}$$

and accordingly the optical refractive index is found as $n_0(\omega) = k(\omega)c\omega^{-1}$:

$$n_0(\omega) = (N_0 + ac\omega^2) + i(K_0 c\omega^{-1} + K_1 c\omega). \tag{3}$$

We see that the coefficients $N_0$ and $a$ define the real part of the optical refractive index $n_0$, whereas $K_0$ and $K_1$ define the imaginary part of $n_0$ associated with the medium absorption. Coefficient $g$ characterizes the Kerr-type nonlinear response, and it is related to the cubic nonlinear susceptibility $n_2$ as [34]

$$g = 2n_2/c. \tag{4}$$

We underline that Eq. (1) is formulated for the electric field $E$ of the optical wave, and it is suitable for theoretical modeling of ultrashort pulse evolution with a very broad spectrum, including the case of pulses with few field oscillations. We note that Eq. (1) can be considered as a form of the cubic generalized Kadomtsev-Petviashvili equation [32]. Below, we will use this equation to model the dynamics of few- and single-period pulses in nonlinear optical media.

Before progressing with our study, it is instructive to discuss a connection between Eq. (1) and the equations for the electric-field envelopes which were originally derived for narrow-band or quasimonochromatic pulses [35]. The envelope equations with additional terms [1,6] are nowadays often used to simulate evolution of pulses with few optical-field oscillations. Since in our study we investigate the process of harmonic generation, it is instructive to derive the envelope equations accounting for the generation of the third optical harmonic. For this purpose, the electric field can be written as

$$E(z,x,y,t) = \tfrac{1}{2}\mathcal{E}_{\omega_0}(z,x,y,t)e^{ik_r(\omega_0)z - i\omega_0 t} + \tfrac{1}{2}\mathcal{E}_{3\omega_0}(z,x,y,t)e^{ik_r(3\omega_0)z - 3i\omega_0 t} + \text{c.c.}, \tag{5}$$

where $\mathcal{E}_{\omega_0}(z,x,y,t)$ and $\mathcal{E}_{3\omega_0}(z,x,y,t)$ are the complex envelopes of quasimonochromatic pulses with the carrier frequencies $\omega_0$ and $3\omega_0$, respectively. After substituting Eq. (5) into Eq. (1) and making simplifications according to the assumption of slowly varying envelopes, we obtain the well-known coupled equations for the envelopes of the fundamental and third-harmonic wave envelopes [35] with additional terms accounting for diffraction:

$$\begin{aligned}
&\frac{\partial \mathcal{E}_{\omega_0}}{\partial z} + k_i(\omega_0)\mathcal{E}_{\omega_0} + \frac{1}{V_{\omega_0}}\frac{\partial \mathcal{E}_{\omega_0}}{\partial t} + i\frac{\beta_{\omega_0}}{2}\frac{\partial^2 \mathcal{E}_{\omega_0}}{\partial t^2} - i\gamma\left[\left(\left|\mathcal{E}_{\omega_0}\right|^2 + 2\left|\mathcal{E}_{3\omega_0}\right|^2\right)\mathcal{E}_{\omega_0} + \left(\mathcal{E}^*_{\omega_0}\right)^2\mathcal{E}_{3\omega_0}e^{i\Delta k_r z}\right] = \frac{i}{2k_0}\Delta_\perp \mathcal{E}_{\omega_0},\\
&\frac{\partial \mathcal{E}_{3\omega_0}}{\partial z} + k_i(3\omega_0)\mathcal{E}_{3\omega_0} + \frac{1}{V_{3\omega_0}}\frac{\partial \mathcal{E}_{3\omega_0}}{\partial t} + i\frac{\beta_{3\omega_0}}{2}\frac{\partial^2 \mathcal{E}_{3\omega_0}}{\partial t^2} - i\gamma\left[3\left(\left|\mathcal{E}_{3\omega_0}\right|^2 + 2\left|\mathcal{E}_{\omega_0}\right|^2\right)\mathcal{E}_{3\omega_0} + \mathcal{E}^3_{\omega_0}e^{-i\Delta k_r z}\right] = \frac{i}{6k_0}\Delta_\perp \mathcal{E}_{3\omega_0},
\end{aligned} \tag{6}$$

where

$$\Delta k_r = k_r(3\omega_0) - 3k_r(\omega_0), \quad V_{\omega_0,3\omega_0} = \left(\frac{\partial k(\omega)}{\partial \omega}\right)^{-1}_{\omega_0,3\omega_0},$$

$$\beta_{\omega_0,3\omega_0} = \left(\frac{\partial^2 k(\omega)}{\partial \omega^2}\right)_{\omega_0,3\omega_0}, \quad \gamma = g\omega_0/4. \tag{7}$$

This illustrates the fact that the model in Eq. (1) is very general. In particular, under appropriate approximations, it can be simplified to obtain the well-known equations for the complex envelopes of multifrequency signals [Eqs. (5) and (6)], while taking into account additional terms which become important for short pulses containing only a few oscillations of the electric field.

Importantly, the physical medium dispersion can be well approximated by the dispersion dependence [Eq. (3)] associated with Eq. (1), since we consider a spectral region away from medium resonances [5,7,10]. As an example, we consider the

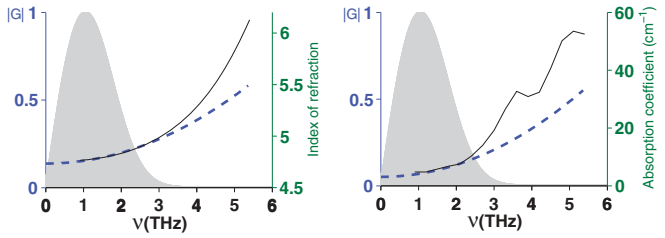


FIG. 2. (Color online) Dispersion of stoichiometric MgO:$LiNbO_3$ crystal: (a) real part of the refractive index $\mathrm{Re}(n_0)$ and (b) absorption coefficient $k_i$ vs the frequency. Solid line: experimental data according to Ref. [42]. Dashed blue line: approximate dependence based on Eq. (3) with parameters $N_0 = 4.734$, $a = 2.224 \times 10^{-38}\ \mathrm{s^3\,cm^{-1}}$, $K_0 = 1.55\ \mathrm{cm^{-1}}$, and $K_1 = 1.32 \times 10^{-26}\ \mathrm{s^2\,cm^{-1}}$. Grey shading: characteristic spectrum ($|G|$) of a single-period pulse with the central frequency 1 THz.

terahertz frequency range. Indeed, generation of single-cycle terahertz pulses with amplitudes exceeding 1 MV/cm was reported [36]. Self-phase modulation of high-energy [37,38] and single-cycle [39–41] THz pulses was recently observed experimentally. We use the experimental data for the frequency dispersion of the optical refractive index in stoichiometric MgO:$LiNbO_3$ crystal from Ref. [42], considering light polarization parallel to the optical axis of the crystal, and determine the values of dispersion parameters $N_0$, $a$, $K_0$, and $K_1$, which provide the best fitting using the least-squares method. The plots in Fig. 2 show that the theoretical dispersion can give an accurate approximation of experimental data in a broad frequency region. This approximation is expected to provide good accuracy for our study of harmonic generation; however, we note that fine structure of the dispersion dependencies would need to be taken into account for the modeling of optical precursors [10].

It is now convenient to normalize Eq. (1), which simplifies the classification of different parameter regions and pulse evolution regimes for the analytical analysis and numerical simulations presented below. Specifically, we introduce the following dimensionless variables:

$$\tilde{E} = \frac{E}{E_0}, \quad \tilde{t} = \frac{4t}{T_0}, \quad \tilde{x} = \frac{x}{r_0}, \quad \tilde{y} = \frac{y}{r_0}, \tag{8}$$

where $E_0$ is a characteristic electric-field amplitude, $T_0$ is the characteristic (central) period of electric-field oscillations, and $r_0$ is the transverse beam width at the input of the nonlinear medium. In new variables, Eq. (1) takes the form

$$\frac{\partial \tilde{E}}{\partial z} + \frac{1}{L_{\mathrm{abs},1}}\tilde{E} + \frac{1}{L_{\mathrm{wave}}}\frac{\partial \tilde{E}}{\partial \tilde{t}} - \frac{1}{L_{\mathrm{abs},2}}\frac{\partial^2 \tilde{E}}{\partial \tilde{t}^2} - \frac{1}{L_{\mathrm{disp}}}\frac{\partial^3 \tilde{E}}{\partial \tilde{t}^3} + \frac{1}{L_{\mathrm{nl}}}\tilde{E}^2\frac{\partial \tilde{E}}{\partial \tilde{t}} = \frac{1}{L_{\mathrm{dif}}}\Delta_\perp \int_{-\infty}^{t} \tilde{E}\,dt'. \tag{9}$$

Here $L_{\mathrm{wave}} = \lambda_0/4$ is the characteristic distance at which the field amplitude varies from zero to a maximum value, $L_{\mathrm{disp}} = \pi^2\lambda_0 N_0/16\Delta n_{\mathrm{disp}}$ is the dispersion length, $L_{\mathrm{dif}} = 8r_0^2/\lambda_0$ is the diffraction length, $L_{\mathrm{nl}} = \lambda_0 N_0/16\Delta n_{\mathrm{nl}}$ is the nonlinear length, $L_{\mathrm{abs},1} = 1/K_0$ and $L_{\mathrm{abs},2} = T_0^2/(16K_1)$ are the absorption lengths, $\lambda_0 = cT_0/N_0$ is the central wavelength, $\Delta n_{\mathrm{disp}} = ac\omega_0^2$ is a modification of the refractive index at the central wavelength due to dispersion, $\Delta n_{\mathrm{nl}} = (1/2)n_2 E_0^2$ is a nonlinearly induced change of the optical refractive index, and $\omega_0 = 2\pi/T_0$ is the central optical frequency. To simplify the notations, in the following we will often omit the tilde symbol (˜) where this does not lead to confusion.

Under the variable normalization according to Eq. (8), the input pulse parameters are effectively scaled to unity. On the other hand, the lengths $L_{\mathrm{nl}}$, $L_{\mathrm{disp}}$, $L_{\mathrm{abs},1}$, $L_{\mathrm{abs},2}$, and $L_{\mathrm{dif}}$ depend on the physical input pulse and medium characteristics, and the relation between these lengths will determine which effects of nonlinearity, dispersion, absorption, or diffraction primarily determine the initial stages of the pulse evolution.

It is useful to provide estimates of the parameters corresponding to practical conditions. As an example, we consider the experimental study of the self-phase modulation of a single-period THz pulse in $LiNbO_3$ crystal [40]. The crystal dispersion corresponding to the experimental spectral region is shown in Fig. 2, which was discussed above. The nonlinear medium coefficient was determined experimentally [40] as $n_2' = 5.4 \times 10^{-12}\ \mathrm{cm^2/W}$, which can be expressed in electromagnetic centimeter-gram-second (CGS) units [43] as $n_2'\ [\mathrm{cm^2/kW}] = (4\pi/3N_0)n_2\ [\mathrm{CGS}]$. The nonlinear self-phase modulation was registered for pulses with intensity $I = 10^8\ \mathrm{W/cm^2}$, which can be expressed in electromagnetic CGS units as $I\ [\mathrm{kW/cm^2}] = (3N_0/8\pi)E_0^2\ [\mathrm{CGS}]$. The central pulse period was $T_0 = 10^{-12}$ s. For the transverse beam width of $r_0 = 10\lambda_0$ (this parameter was not specified in Ref. [40]), we obtain $L_{\mathrm{nl}} \simeq 35$ mm, $L_{\mathrm{disp}} \simeq 7$ mm, $L_{\mathrm{abs},1} \simeq 7$ mm, $L_{\mathrm{abs},2} \simeq 47$ mm, and $L_{\mathrm{dif}} \simeq 51$ mm. These length values can be changed by varying the input intensity and beam width.

In the following we analyze the cases when $L_{\mathrm{nl}}, L_{\mathrm{disp}}, L_{\mathrm{dif}} \ll L_{\mathrm{abs},1}, L_{\mathrm{abs},2}$. Considering such conditions, which physically correspond to spectral regions away from medium resonances [5,7,10], we neglect the effects of absorption.

## III. PULSE PROPAGATION WITH WEAK DISPERSION AND DIFFRACTION

### A. Perturbation theory

First we analyze the case when the dispersion and diffraction lengths are much larger than the nonlinear length:

$$L_{\mathrm{nl}} \ll L_{\mathrm{disp}}, L_{\mathrm{dif}}. \tag{10}$$

Then, considering the propagation distances $z < L_{\mathrm{disp}}, L_{\mathrm{dif}}$, we neglect the effects of dispersion and diffraction and simplify Eq. (9) as

$$\frac{\partial E}{\partial z} + \frac{1}{L_{\mathrm{wave}}}\frac{\partial E}{\partial t} + \frac{1}{L_{\mathrm{nl}}}E^2\frac{\partial E}{\partial t} = 0. \tag{11}$$

We now obtain an approximate solution of Eq. (11) using Picard's method of successive approximations [44]. We consider $L_{\mathrm{wave}}/L_{\mathrm{nl}}$ as a small parameter and seek approximate solutions in the form

$$E = E^{(0)} + \frac{L_{\mathrm{wave}}}{L_{\mathrm{nl}}}E^{(1)} + \left(\frac{L_{\mathrm{wave}}}{L_{\mathrm{nl}}}\right)^2 E^{(2)} + \cdots. \tag{12}$$

Keeping the first two terms in the expansion over the small parameter, we obtain the following equations:

$$\frac{\partial E^{(0)}}{\partial z}+\frac{1}{L_{\rm wave}}\frac{\partial E^{(0)}}{\partial t}=0, \tag{13}$$

$$\frac{\partial E^{(1)}}{\partial z}+\frac{1}{L_{\rm wave}}\frac{\partial E^{(1)}}{\partial t}+\frac{(E^{(0)})^2}{L_{\rm nl}}\frac{\partial E^{(0)}}{\partial t}=0. \tag{14}$$

Solution of Eq. (13) has the form [45]

$$E^{(0)}(z,t)=E^{(0)}\left(t-\frac{z}{L_{\rm wave}}\right). \tag{15}$$

Solution of Eq. (14) can be expressed in quadratures after making a variable transformation $z'=z/L_{\rm wave}$ and $\tau=t-z/L_{\rm wave}$:

$$\begin{aligned}E^{(1)}(z',\tau)&=-\frac{1}{3}\int_{z'_0}^{z'}\frac{\partial}{\partial\tau}[E^{(0)}(\tau)]^3dz''\\&=-\frac{1}{3}\left\{\frac{\partial}{\partial\tau}[E^{(0)}(\tau)]^3\right\}(z'-z'_0),\end{aligned} \tag{16}$$

where $z'_0$ is the boundary of the nonlinear medium. With no loss of generality, we set $z'_0=0$ in the following.

### B. Single-period pulse evolution and harmonic generation

We now consider an evolution of an incident one-period pulse of the form

$$E^{(0)}(0,t)=E_0\left(\frac{t}{\tau_p}\right)\exp\left(-\frac{t^2}{\tau_p^2}\right), \tag{17}$$

where $E_0$ is the characteristic field amplitude and $\tau_p$ is the input pulse duration. The expression in Eq. (17) provides a good approximation of terahertz emission from semiconductor interfaces illuminated with femtosecond optical pulses [46]. The temporal spectrum of such a pulse is

$$\begin{aligned}G^{(0)}(0,\omega)&=\int_{-\infty}^{\infty}E^{(0)}(0,t)\,e^{-i\omega t}dt\\&=-i\frac{\sqrt{\pi}}{2}E_0\tau_p^2\omega\exp\left(-\tau_p^2\omega^2/4\right).\end{aligned} \tag{18}$$

According to this expression, the spectral peak is at the frequency $\omega_{\rm max}=\sqrt{2}/\tau_p$.

We now apply the normalization according to Eq. (8) with $T_0=2\pi/\omega_{\rm max}=\sqrt{2}\pi\tau_p$. Then, the normalized field of the single-period pulse and its spectrum is written as

$$\tilde{E}^{(0)}(0,\tilde{t})=\frac{\pi}{2\sqrt{2}}\tilde{t}\exp\left(-\frac{\pi^2\tilde{t}^2}{8}\right), \tag{19}$$

$$\begin{aligned}\tilde{G}^{(0)}(0,\tilde{\omega})&=\int_{-\infty}^{\infty}\tilde{E}^{(0)}(0,\tilde{t})\,e^{-i\tilde{\omega}\tilde{t}}d\tilde{t}\\&=-i4\pi^{-3/2}\tilde{\omega}\exp(-2\tilde{\omega}^2\pi^{-2}).\end{aligned} \tag{20}$$

The normalized frequency is defined as $\tilde{\omega}=\omega T_0/4=\omega\sqrt{2}\pi\tau_p/4$. Based on Eq. (20), we determine the position of the maximum of spectral distribution as $\tilde{\omega}_{\rm max}=\pi/2$. It is therefore convenient to introduce the notation

$$\Omega=\omega/\omega_{\rm max}=\tilde{\omega}/\tilde{\omega}_{\rm max}=2\tilde{\omega}/\pi, \tag{21}$$

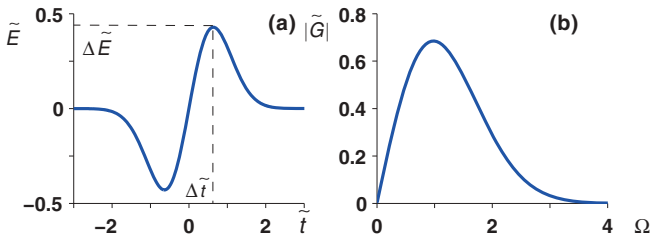


FIG. 3. (Color online) (a) Electric-field profile of a single-cycle light pulse defined by Eq. (19) and (b) its spectrum according to Eq. (20).

such that the normalized frequency $\Omega=1$ corresponds to the spectral peak, and we will use $\Omega$ as the frequency axis in plots. We show the electric-field profile and its spectrum according to Eqs. (19) and (20) in Figs. 3(a) and 3(b), respectively. We calculate the scale of the field amplitude change between the pulse center and the main field maximum as $\Delta\tilde{E}/\Delta\tilde{t}\approx 0.7$, where $\Delta\tilde{t}$ is the position of the maximum and $\Delta\tilde{E}$ is the peak amplitude as illustrated in Fig. 3(a). We note that the total field oscillation $2\Delta\tilde{E}$, the central field gradient, the spectral peak frequency, and the peak spectral amplitude are all of the order of unity, which indicates that our choice of normalization is suitable for such single-cycle optical pulses and justifies the classification of pulse dynamics based on the normalized characteristic lengths $L_{\rm disp}$, $L_{\rm dif}$, and $L_{\rm nl}$.

We calculate the first-order correction to the pulse profile by substituting Eq. (19) into Eq. (16),

$$\tilde{E}^{(1)}(z',\tau)=-\frac{\pi^3z'\tau^2}{16\sqrt{2}}\left(1-\frac{\pi^2\tau^2}{4}\right)e^{-3\pi^2\tau^2/8}, \tag{22}$$

and then we find its spectrum:

$$\begin{aligned}\tilde{G}^{(1)}(z',\tilde{\omega})=&-\frac{2\sqrt{\pi}}{9\sqrt{3}\pi^2}z'\tilde{\omega}^2\left[1-\left(\frac{2\tilde{\omega}}{3\pi}\right)^2\right]\\&\times\exp\left(-\frac{2\tilde{\omega}^2}{3\pi^2}\right)e^{-i\tilde{\omega}z'}.\end{aligned} \tag{23}$$

We show these corrections in Figs. 4(a) and 4(b). According to Eq. (23) the nonlinearly induced spectral correction vanishes at the third harmonic of the input pulse spectral peak frequency, $\tilde{\omega}=3\pi/2=3\tilde{\omega}_{\rm max}$, and this is also clearly visible in Fig. 4(b). This is a remarkably surprising result, since the third-harmonic generation is one of the fundamental effects in optical media with Kerr-type nonlinearity. However, our finding indicates that the process of third-harmonic generation can be dramatically modified for single-period optical pulses.

We combine, according to Eq. (12), the first two perturbation series terms, which define the total iterative solution:

$$\begin{aligned}\tilde{E}(z',\tau)&=\tilde{E}^{(0)}(\tau)+\frac{L_{\rm wave}}{L_{\rm nl}}\tilde{E}^{(1)}(z',\tau)\\&=\frac{\pi\tau}{2\sqrt{2}}\exp\left(-\frac{\pi^2\tau^2}{8}\right)\left[1-\frac{L_{\rm wave}}{L_{\rm nl}}\frac{\pi^2z'}{8}\tau\right.\\&\left.\times\left(1-\frac{\pi^2\tau^2}{4}\right)\exp\left(-\frac{\pi^2\tau^2}{4}\right)\right],\end{aligned} \tag{24}$$

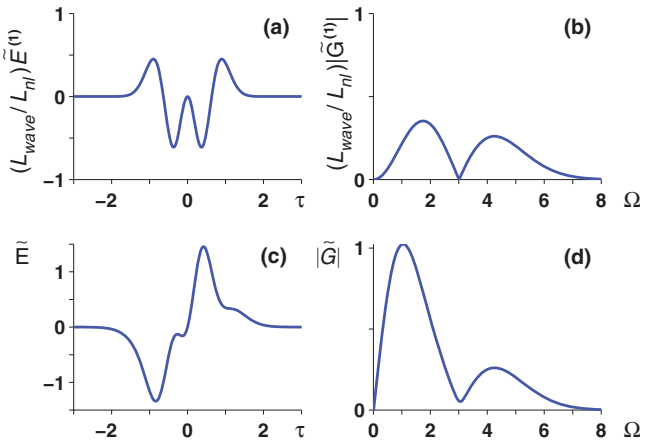


FIG. 4. (Color online) Nonlinearly induced change of temporal and spectral structures of a single-cycle optical pulse. (a and b) Nonlinearly induced corrections to (a) field $(L_{\rm wave}/L_{\rm nl})\tilde{E}^{(1)}$ and (b) modulus of spectrum $(L_{\rm wave}/L_{\rm nl})\tilde{G}^{(1)}$ calculated based on Eqs. (22) and (23), respectively. (c and d) The total field and spectrum resulting field according to Eqs. (24) and (25), respectively. The propagation distance is $z' = 7$ and $L_{\rm wave}/L_{\rm nl} = 0.5$.

which is found as

$$\begin{aligned}\tilde{G}(z',\tilde{\omega}) &= \tilde{G}^{(0)}(0,\tilde{\omega}) + \frac{L_{\rm wave}}{L_{\rm nl}}\tilde{G}^{(1)}(z',\tilde{\omega}) \\ &= -i\frac{4\sqrt{\pi}}{\pi^2}\tilde{\omega}\exp(-i\tilde{\omega}z')\exp(-2\tilde{\omega}^2/\pi^2) \\ &\quad\times\left\{1 - i\frac{L_{\rm wave}}{L_{\rm nl}}\frac{z'\tilde{\omega}}{18\sqrt{3}}\left[1 - \left(\frac{2\tilde{\omega}}{3\pi}\right)^2\right]e^{4\tilde{\omega}^2/3\pi^2}\right\}.\end{aligned} \tag{25}$$

The characteristic pulse profile and spectrum calculated according to these expressions are shown in Figs. 4(c) and 4(d), respectively. Results are plotted for $L_{\rm wave}/L_{\rm nl} = 0.5$. Although this parameter should be small for the perturbation series analysis to be formally valid, we choose a relatively large value for it to make the difference between the perturbed [Figs. 4(c) and 4(d)] and input [Figs. 3(a) and 3(b)] pulse profile and spectrum more clearly visible in the plots.

We observe in Fig. 4(c) that the field maxima and minima get delayed in time due to nonlinear self-action, whereas in linear media and in the absence of dispersion the pulse shape would be the same as at the input (note that we plot in the moving-frame coordinates) [cf. Fig. 3(a)]. The overall shape of the pulse also gets distorted. In the pulse spectrum, the self-action is evident as the generation of higher frequencies is visible in Fig. 4(d), whereas in linear media the modulus of the spectrum would be the same as at the input [cf. Fig. 3(b)]. We again emphasize that the nonlinear spectral correction vanishes at the third harmonic of the peak input spectral frequency, and the maximum of the correction appears at around $\Omega \approx 4.5$ [see Fig. 4(b)].

### C. Field evolution and harmonic generation for different pulse durations

After revealing the intriguing effect of suppressed third-harmonic generation for single-cycle optical pulses, we perform a systematic investigation of the effect of input pulse duration on generation of optical harmonics. For this purpose, we consider input pulses with Gaussian envelopes:

$$E^{(0)}(0,t) = E_0\exp\left(-t^2/\tau_p^2\right)\sin(\omega_0 t), \tag{26}$$

where $\tau_p$ is the pulse duration and $\omega_0$ is the central frequency. The pulse spectrum is found as

$$\begin{aligned}G^{(0)}(0,\omega) = \frac{\sqrt{\pi}E_0\tau_p}{2i}&\left\{\exp\left[-\tau_p^2(\omega-\omega_0)^2/4\right]\right. \\ &\left.-\exp\left[-\tau_p^2(\omega+\omega_0)^2/4\right]\right\}.\end{aligned} \tag{27}$$

In normalized units according to Eq. (8), the pulse profile and spectrum are defined as

$$\tilde{E}^{(0)}(0,\tilde{t}) = \exp\left[-\left(\frac{T_0\tilde{t}}{4\tau_p}\right)^2\right]\sin\left(\frac{\pi}{2}\tilde{t}\right), \tag{28}$$

$$\begin{aligned}\tilde{G}^{(0)}(0,\tilde{\omega}) = \frac{2\sqrt{\pi}\tau_p}{iT_0}&\left\{\exp\left[-\frac{4\tau_p^2(\tilde{\omega}-\pi/2)^2}{T_0^2}\right]\right. \\ &\left.-\exp\left[-\frac{4\tau_p^2(\tilde{\omega}+\pi/2)^2}{T_0^2}\right]\right\}.\end{aligned} \tag{29}$$

We plot the characteristic pulse profiles and spectra for different pulse durations in Fig. 5. For a long pulse containing many field oscillations under the envelope [Fig. 5(a)], the spectrum is confined around the central frequency [Fig. 5(b)]. For a shorter pulse which contains only one strong field oscillation [Fig. 5(c)], the spectrum is much broader [Fig. 5(d)]. The pulse profile and spectrum in the latter case are very similar to those of a single-period pulse considered in the previous section [cf. Figs. 3(a) and 3(b)]. We also present the pulse profiles and spectra for a range of durations using density plots in Figs. 6(a) and 6(b), respectively.

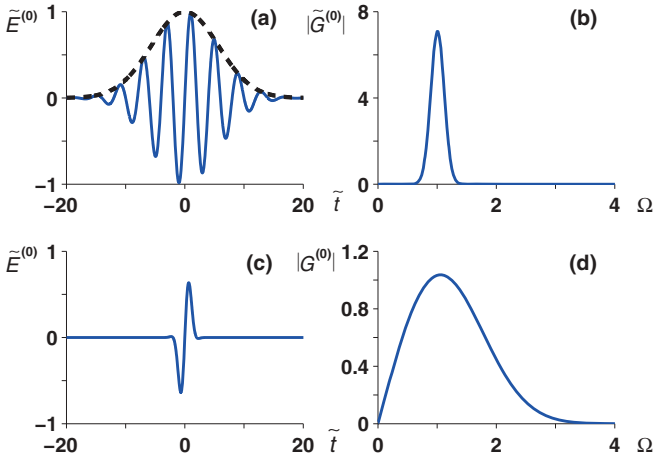


FIG. 5. (Color online) (a and c) Field of a Gaussian optical pulse and (b and c) the corresponding optical spectrum calculated according to Eqs. (28) and (29), respectively. The normalized pulse duration $\tau_p/T_0$ is (a and b) 2 and (c and d) 0.3. The Gaussian pulse envelope is shown by a dashed line in (a).

Next, we determine the nonlinear correction to the pulse profile by substituting Eq. (28) into Eq. (16):

$$\tilde{E}^{(1)}(z',\tau) = \exp\left(-\frac{3T_0^2\tau^2}{16\tau_p^2}\right) z' \left[\frac{3T_0^2\tau}{32\tau_p^2}\sin\left(\frac{\pi}{2}\tau\right) - \frac{\pi}{8}\cos\left(\frac{\pi}{2}\tau\right) - \frac{T_0^2\tau}{32\tau_p^2}\sin\left(\frac{3\pi}{2}\tau\right) + \frac{\pi}{8}\cos\left(\frac{3\pi}{2}\tau\right)\right], \tag{30}$$

and its spectrum is

$$\tilde{G}^{(1)}(z',\tilde{\omega}) = -\sqrt{\frac{\pi}{3}}\frac{\tau_p}{6T_0} z'\tilde{\omega}\exp(-i\tilde{\omega}z') \left\{3\exp\left[-\frac{\tau_p^2(2\tilde{\omega}-\pi)^2}{3T_0^2}\right] - 3\exp\left[-\frac{\tau_p^2(2\tilde{\omega}+\pi)^2}{3T_0^2}\right] - \exp\left[-\frac{\tau_p^2(2\tilde{\omega}-3\pi)^2}{3T_0^2}\right] + \exp\left[-\frac{\tau_p^2(2\tilde{\omega}+3\pi)^2}{3T_0^2}\right]\right\}. \tag{31}$$

We show the nonlinear corrections to the pulse profile and spectrum in Figs. 6(c) and 6(d), respectively. We see that the profile correction [Fig. 6(c)] has a different (even) symmetry compared to the odd input pulse profile [Fig. 6(a)], which would lead to the distortion of the pulse profile in nonlinear medium. The spectral correction has two maxima, and we show the frequency where the correction completely vanishes with the white line in Fig. 6(d). We see that, for a long pulse duration (e.g., $\tau_p/T_0 = 2$), there is no second-harmonic generation while the third harmonic is generated efficiently, which fully agrees with the well-known results for quasimonochromatic pulses. However, as the pulse duration is reduced, the spectral maximum and minimum get shifted to higher frequencies. For a pulse duration of $\tau_p/T_0 \approx 0.29$, the third-harmonic generation vanishes, and this case corresponds to the situation which was identified in the previous section.

To confirm our predictions based on analytical perturbation theory, we perform direct numerical simulations of the model Eq. (9). We perform a series of simulations for different input pulse durations and summarize results in Fig. 7. We choose the propagation distance equal to the nonlinear length, to check the pulse evolution when nonlinear effects are very strong, going beyond the formal applicability of the perturbation theory. The calculated output pulse field and spectrum are presented in Figs. 7(a) and 7(b), respectively. We then find the differences between the output and input profiles and spectra, which are shown in Figs. 7(c) and 7(d), respectively. We observe that the nonlinearly induced pulse change predicted analytically [Fig. 6(c)] shows a very good qualitative agreement with the numerical results [Fig. 7(c)]. In the spectrum, numerical modeling shows the generation of higher optical harmonics [Fig. 7(d)], which occurs due to cascaded nonlinear processes which were not taken account in the analytical analysis [Fig. 6(d)]. Nevertheless, we find that the key analytical prediction of harmonic suppression at certain harmonics remains—we mark those frequencies with the white line in Fig. 7(d), and this line position closely resembles the analytical dependence in Fig. 6(d).

The analytical and numerical results presented in this section demonstrate that harmonic generation very strongly depends on the pulse duration: on the one hand, higher harmonics are generated, yet on the other hand the generation of intermediate harmonics can become completely suppressed.

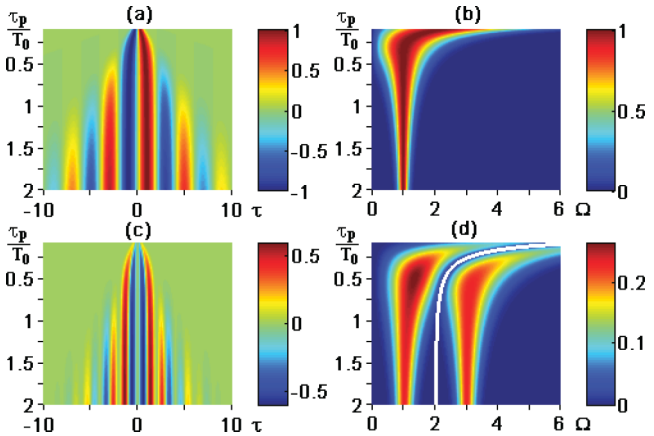


FIG. 6. (Color online) (a and b) The Gaussian pulse (a) field and (b) spectrum vs the normalized duration $\tau_p/T_0$ according to Eqs. (28) and (29), respectively. (c and d) Nonlinearly induced corrections to the pulse (c) field and (d) spectrum vs the normalized duration according to Eqs. (30) and (31), respectively. The white line in (d) marks the minimum of the spectral correction.

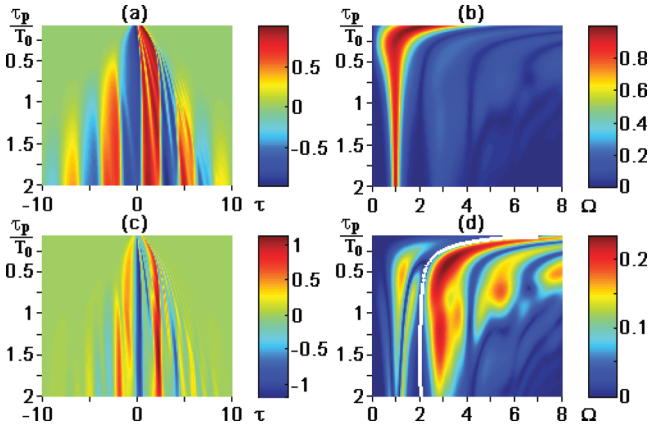


FIG. 7. (Color online) Numerical simulation of pulse propagation for different input durations $\tau_p/T_0$. (a and b) The output pulse (a) field and (b) spectrum. (c and d) Differences between the output and input (c) field and (d) spectrum. The white line in (d) marks the minimum of the spectral correction. Parameters are $L_{\rm nl} = 7$ mm and $L_{\rm disp} = L_{\rm dif} = \infty$. Propagation distance is $z = 7$ mm.

## IV. EFFECT OF DISPERSION ON NONLINEAR PULSE SELF-ACTION

In the previous section, we have analyzed pulse self-action while under the conditions when the dispersion and diffraction effects can be neglected. We now consider the effect of dispersion, while still considering the propagation of wide beams which exhibit weak diffraction:

$$L_{\rm nl} \sim L_{\rm disp} \ll L_{\rm dif}. \tag{32}$$

Under such conditions, the model Eq. (9) can be simplified by neglecting diffraction:

$$\frac{\partial E}{\partial z} + \frac{1}{L_{\rm wave}}\frac{\partial E}{\partial t} - \frac{1}{L_{\rm disp}}\frac{\partial^3 E}{\partial t^3} + \frac{1}{L_{\rm nl}}E^2\frac{\partial E}{\partial t} = 0. \tag{33}$$

This equation is known in the literature as the Korteweg-de Vries equation, and it was previously derived for the intense optical pulses propagating in media with Kerr nonlinearity in the regime of normal group-velocity dispersion in Ref. [47] and then further analyzed in a number of papers (see the recent review [13]).

We perform numerical simulations for the case when the propagation distance is equal to both the nonlinear and dispersion lengths, such that nonlinearity and dispersion both play a strong role. We calculate the dependence of the output field and spectrum on the input pulse duration, presented in Figs. 8(a) and 8(b), respectively. We also perform simulations in the linear regime (taking $L_{\rm nl} = \infty$) and calculate a difference between the nonlinear and linear outputs, which is shown in Figs. 8(c) and 8(d). Similar to the case of zero dispersion, we find that the nonlinear spectral correction vanishes for the second harmonic for long pulses. For shorter pulses, the zero of spectral correction shifts to higher frequencies, as marked with the white line in Fig. 8(d). Additionally, there appear several minima in the spectral correction, and one such minimum is shown by another white line in Fig. 8(d). Therefore, the zero of the third harmonic can appear for several

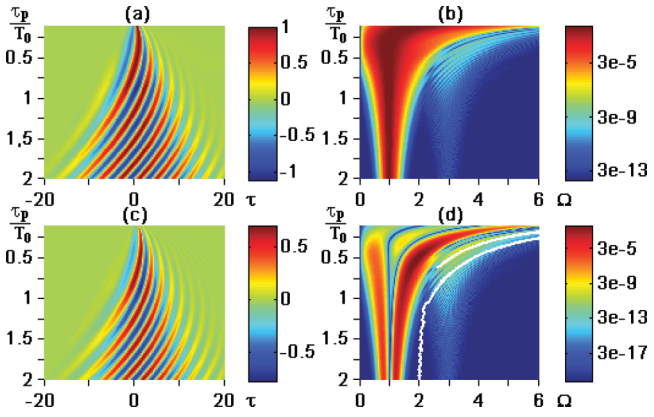


FIG. 8. (Color online) Numerical simulation of pulse propagation for different input durations $\tau_p/T_0$. (a and b) The output pulse (a) field and (b) spectrum under the effects of nonlinear self-action and dispersion, $L_{\rm nl} = L_{\rm disp} = 7$ mm. (c and d) Nonlinear corrections for the output (c) field and (d) spectrum calculated as a difference between results in (a and b) and linear simulations when $L_{\rm nl} = \infty$. For all the plots $L_{\rm dif} = \infty$, and the propagation distance is $z = 7$ mm. The white lines in (d) mark the minima of the spectral correction.

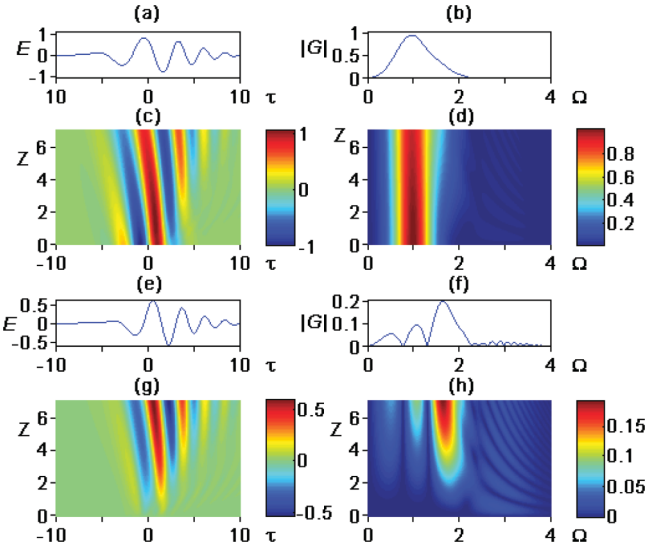


FIG. 9. (Color online) (a and c) Electric fields and (b and d) spectra for the case $L_{\rm disp} = 7$ mm, $L_{\rm nl} = 7$ mm. (e–h) The nonlinear correction to the fields and output spectra for the cases $L_{\rm disp} = 7$ mm, $L_{\rm nl} = 7$ mm and $L_{\rm disp} = 7$ mm, $L_{\rm nl} = \infty$. (a, b, e, and f) Output profiles at $z = 7$ mm. (c, d, g, and h) Density plots showing evolution along the propagation direction $z$. For all the plots the input pulse duration is $\tau_p/T_0 \cong 0.71$.

pulse durations, which is different from the case of zero dispersion considered in the previous case when third-harmonic generation vanishes for one particular value of the pulse duration. Here, we identify that the third-harmonic component vanishes, for example, for the normalized input pulse duration $\tau_p/T_0 \approx 0.71$. This value is different than in the case of zero dispersion considered in the previous section due to dispersion.

We now perform a detailed analysis of harmonic generation during the propagation of the pulse with duration $\tau_p/T_0 \approx 0.71$. We show the output field and spectrum in Figs. 9(a) and 9(b) and their evolution along the propagation direction in Figs. 9(c) and 9(d). We also present the differences between the nonlinear and linear propagation in Figs. 9(e)–9(h). We observe a complex pulse transformation due to the combined effects of dispersion and nonlinearity. We observe that the third-harmonic generation is at a series of positions along the propagation direction [see Fig. 9(h)].

Finally, we perform a series of numerical simulations for varying dispersion length, while keeping other parameters fixed. The results are presented in Fig. 10. We see that dispersion leads to increased pulsed broadening, and the electric-field profile becomes strongly asymmetric [see Fig. 10(a)]. The effect of dispersion on harmonic generation is visualized in Fig. 10(d). We see that as the dispersion is increased the maximum of spectral nonlinear correction is moved to lower frequencies. This occurs because dispersion leads to pulse broadening, and for longer pulses generation of higher harmonics is less efficient. Another observation is that for the chosen pulse and nonlinearity parameters the third-harmonic generation is suppressed for zero dispersion; however, for an intermediate dispersion value the spectral maximum becomes centered exactly at the third harmonic. Therefore, an interplay

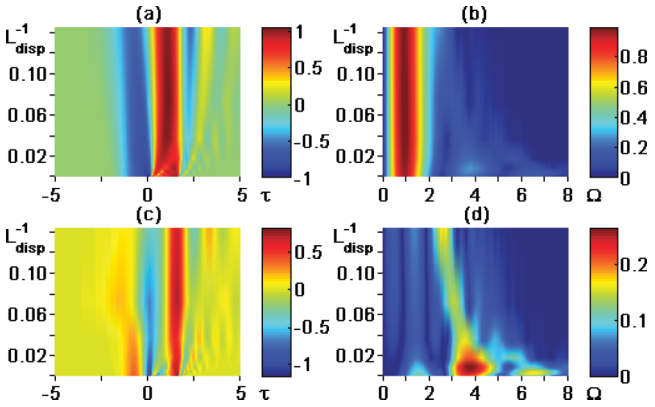


FIG. 10. (Color online) Numerical simulation of pulse propagation for different dispersion strengths defined as inverse dispersion length $L_{\text{disp}}^{-1}$. (a and b) The output pulse (a) field and (b) spectrum under the effects of nonlinear self-action, $L_{\text{nl}} = 7$ mm. (c and d) Nonlinear corrections for the output (c) field and (d) spectrum calculated as a difference between results in (a and b) and linear simulations when $L_{\text{nl}} = \infty$. For all the plots $L_{\text{dif}} = \infty$, the pulse duration is $\tau_p/T_0 = 0.3$, and the propagation distance is $z = 7$ mm.

between dispersion and nonlinearity can offer rich possibilities to suppress or enhance the generation of particular optical harmonics by ultrashort pulses.

## V. SPATIOTEMPORAL NONLINEAR PULSE DYNAMICS

We now analyze the spatiotemporal pulse dynamics and harmonic generation under the combined effects of nonlinearity, temporal dispersion, and spatial diffraction. Specifically, we consider the regime when $L_{\text{disp}} \sim L_{\text{dif}} \sim L_{\text{nl}}$.

First, we consider the propagation of an ultrashort pulse when $L_{\text{disp}} = L_{\text{nl}} = L_{\text{dif}}$ and present characteristic simulation results in Fig. 11. We observe a strong distortion of the wave front, which is a signature of spatial self-focusing [see the field profiles in Figs. 11(c) and 11(e)]. The corresponding spectra are presented in Figs. 11(d) and 11(f). We observe that the beam is strongly broadened at low frequencies, which is a feature of linear diffraction. On the other hand, higher-harmonic generation occurs on the beam axis, where optical intensity is the highest. We notice the presence of several peaks and minima in the higher-harmonic amplitudes, which is due to the interplay of dispersion and nonlinearity, as we identified in the previous section. We note that the multipeak spectrum is a generic feature, which also appeared in previous simulations for the case of anomalous dispersion [32], whereas in our analysis we consider normal dispersion.

Next, we analyze the same pulse propagation, but with increased intensity corresponding to a shorter nonlinear length of $L_{\text{nl}} = 7$ mm (see Fig. 12). We see that the self-focusing and harmonic generation is increased compared to the previous example in Fig. 11. Interestingly, for an intermediate propagation length the third-harmonic generation is suppressed [Fig. 12(d)], whereas the third harmonic appears at a longer distance [Fig. 12(f)]. This is also a feature identified in the previous section as due to the interplay of dispersion and nonlinearity.

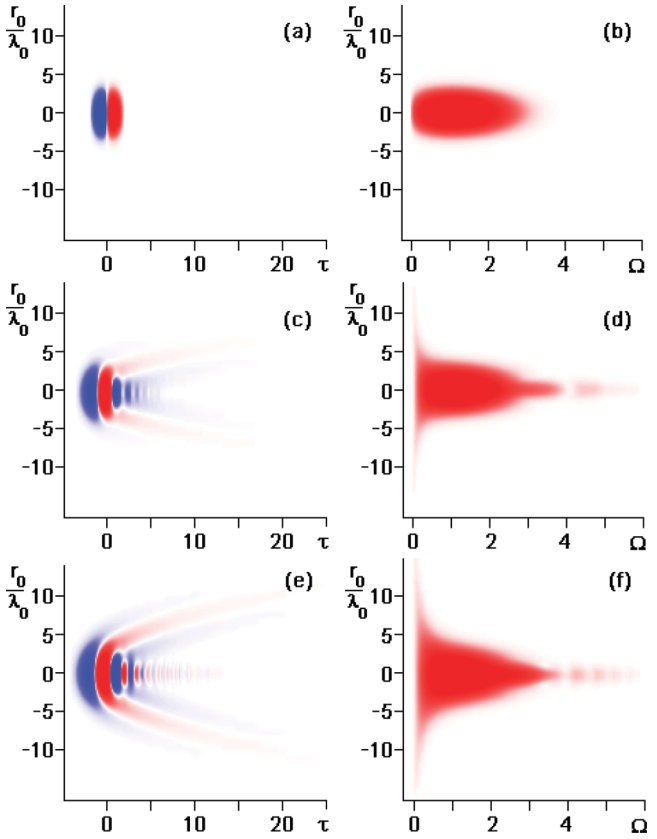


FIG. 11. (Color online) (a, c, and e) Spatiotemporal evolution of the electric-field and (b, d, and f) corresponding spatiospectral profiles of the spectrum modulus at distances (a and b) $z = 0$, (c and d) $z = 15$ mm, and (e and f) $z = 30$ mm. Input pulse duration is $\tau_p/T_0 = 0.3$ and the width of the Gaussian transverse profile is $r_0 = 8.3\lambda_0$. Parameters are $L_{\text{disp}} = L_{\text{nl}} = L_{\text{dif}} = 35$ mm.

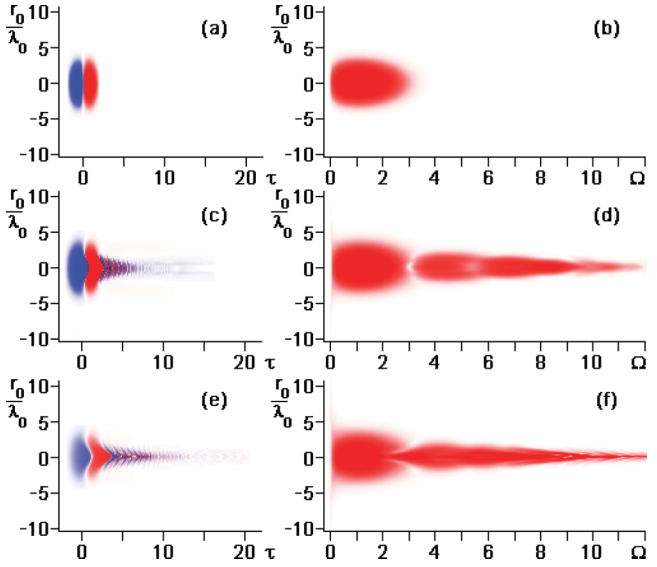


FIG. 12. (Color online) (a, c, and e) Spatiotemporal evolution of the electric-field and (b, d, and f) corresponding spatiospectral profiles of the spectrum modulus at distances (a and b) $z = 0$, (c and d) $z = 4$ mm, and (e and f) $z = 8$ mm. Input pulse duration is $\tau_p/T_0 = 0.3$ and the width of the Gaussian transverse profile is $r_0 = 8.3\lambda_0$. Parameters are $L_{\text{disp}} = L_{\text{dif}} = 35$ mm and $L_{\text{nl}} = 7$ mm.

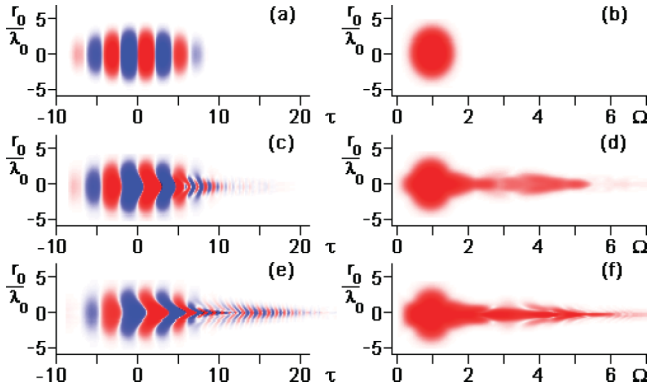


FIG. 13. (Color online) (a, c, and e) Spatiotemporal evolution of the electric-field and (b, d, and f) corresponding spatiospectral profiles of the spectrum modulus at distances (a and b) $z = 0$, (c and d) $z = 2.5$ mm, and (e and f) $z = 5$ mm. Input pulse duration is $\tau_p/T_0 = 1.0$ and the width of the Gaussian transverse profile is $r_0 = 8.3\lambda_0$. Parameters are $L_{\rm disp} = L_{\rm dif} = 35$ mm and $L_{\rm nl} = 7$ mm.

Finally, we perform a comparison with a longer pulse propagation (see Fig. 13). In this case, the lower frequencies are essentially absent [see Figs. 13(b), 13(d), and 13(f)]. The higher-harmonic generation naturally occurs at the beam axis.

## VI. CONCLUSION

We have analyzed the effects of weak nonlinearity and dispersion on the spatiotemporal dynamics of few-cycle optical pulses, emphasizing the interplay of different competitive spatial and temporal scales. In particular, we have discussed nonlinearity-induced self-phase modulation, generation of higher harmonics by a few-cycle pulse, and the effects of the beam diffraction. We have demonstrated that in dispersive and diffractive nonlinear media the nonlinear equations governing the spatiotemporal propagation of short pulses can be reduced to the cubic nonlinear Schrödinger equation only in the special limit of long pulses. Using a general model, we have studied self-action effects of few-cycle pulses and described, both analytically and numerically, the pulse self-modulation and self-focusing, including the transformation of the spectral density and harmonic generation in the cases of weak and strong dispersion.

## ACKNOWLEDGMENTS

This work was supported by grants from the Ministry of Education and Science of the Russian Federation (projects No. 14.B37.21.0907 and No. 16.740.11.0459), the Russian Foundation for Basic Research (Grant No. 11-02-01346-a), and the Australian Research Council programs (including Future Fellowship No. FT100100160).

[1] T. Brabec and F. Krausz, Rev. Mod. Phys. **72**, 545 (2000).
[2] M. Wegener, *Extreme Nonlinear Optics: An Introduction* (Springer-Verlag, Berlin, 2005).
[3] E. Goulielmakis *et al.*, Science **320**, 1614 (2008).
[4] F. Krausz and M. Ivanov, Rev. Mod. Phys. **81**, 163 (2009).
[5] K. E. Oughstun and H. Xiao, Phys. Rev. Lett. **78**, 642 (1997).
[6] T. Brabec and F. Krausz, Phys. Rev. Lett. **78**, 3282 (1997).
[7] H. Xiao and K. E. Oughstun, J. Opt. Soc. Am. B **16**, 1773 (1999).
[8] M. S. Syrchin, A. M. Zheltikov, and M. Scalora, Phys. Rev. A **69**, 053803 (2004).
[9] S. Amiranashvili and A. Demircan, Phys. Rev. A **82**, 013812 (2010).
[10] C. L. Palombini and K. E. Oughstun, Opt. Express **18**, 23104 (2010).
[11] L. Berge and S. Skupin, Phys. Rev. E **71**, 065601 (2005).
[12] L. Berge and S. Skupin, Phys. Rev. Lett. **100**, 113902 (2008).
[13] H. Leblond and D. Mihalache, Rom. Rep. Phys. **63**, 1254 (2011).
[14] N. N. Akhmediev, I. V. Melnikov, and A. V. Nazarkin, "Propagation of a femtosecond optical pulse in transparency region of a nonlinear medium," Sbornik Kratkie Soobshcheniya Po Fizike, an Sssr, Fizicheskii Institut Im. P. N. Lebedeva, no. 2, pp. 49–51 (1989) [Sov. Phys.-Lebedev Inst. Rep. (USA), no. 2, pp. 66–69 (1989)].
[15] E. M. Belenov and A. V. Nazarkin, JETP Lett. **51**, 288 (1990).
[16] I. V. Melnikov, D. Mihalache, F. Moldoveanu, and N. C. Panoiu, JETP Lett. **65**, 393 (1997).
[17] I. V. Melnikov, D. Mihalache, F. Moldoveanu, and N. C. Panoiu, Phys. Rev. A **56**, 1569 (1997).
[18] T. Schafer and C. E. Wayne, Physica D **196**, 90 (2004).
[19] H. Leblond, S. V. Sazonov, I. V. Mel'nikov, D. Mihalache, and F. Sanchez, Phys. Rev. A **74**, 063815 (2006).
[20] H. Leblond and D. Mihalache, Phys. Rev. A **79**, 063835 (2009).
[21] S. Amiranashvili, A. G. Vladimirov, and U. Bandelow, Eur. Phys. J. D **58**, 219 (2010).
[22] H. Leblond, H. Triki, and D. Mihalache, Phys. Rev. A **84**, 023833 (2011).
[23] H. Leblond, H. Triki, F. Sanchez, and D. Mihalache, Opt. Commun. **285**, 356 (2012).
[24] S. A. Kozlov and S. V. Sazonov, JETP **84**, 221 (1997).
[25] V. G. Bespalov, S. A. Kozlov, Y. A. Shpolyansky, and I. A. Walmsley, Phys. Rev. A **66**, 013811 (2002).
[26] S. V. Sazonov and V. A. Khalyapin, Quantum Electron. **34**, 1057 (2004).
[27] A. N. Berkovsky, S. A. Kozlov, and Y. A. Shpolyanskiy, Phys. Rev. A **72**, 043821 (2005).
[28] A. G. Litvak, V. A. Mironov, and S. A. Skobelev, JETP Lett. **82**, 105 (2005).
[29] A. A. Balakin, A. G. Litvak, V. A. Mironov, and S. A. Skobelev, Phys. Rev. A **78**, 061803 (2008).
[30] A. A. Balakin, A. G. Litvak, V. A. Mironov, and S. A. Skobelev, Phys. Rev. A **80**, 063807 (2009).
[31] H. Leblond, D. Kremer, and D. Mihalache, Phys. Rev. A **80**, 053812 (2009).
[32] H. Leblond, D. Kremer, and D. Mihalache, Phys. Rev. A **81**, 033824 (2010).

[33] K. Glasner, M. Kolesik, J. V. Moloney, and A. C. Newell, Int. J. Optics **2012**, 898 (2012).
[34] V. G. Bespalov, S. A. Kozlov, and Y. A. Shpolyanskii, J. Opt. Technol. **67**, 303 (2000).
[35] G. P. Agrawal, *Nonlinear Fiber Optics*, 4th ed. (Academic, New York, 2006).
[36] H. Hirori, A. Doi, F. Blanchard, and K. Tanaka, Appl. Phys. Lett. **98**, 091106 (2011).
[37] J. Hebling, K. L. Yeh, M. C. Hoffmann, and K. A. Nelson, IEEE J. Sel. Top. Quantum Electron. **14**, 345 (2008).
[38] J. A. Fulop, L. Palfalvi, G. Almasi, and J. Hebling, J. Infrared Millim. Terahertz Waves **32**, 553 (2011).
[39] H. Wen, M. Wiczer, and A. M. Lindenberg, Phys. Rev. B **78**, 125203 (2008).
[40] J. Hebling, M. C. Hoffmann, K. L. Yeh, G. Tóth, and K. A. Nelson, in *Ultrafast Phenomena XVI*, edited by P. Corkum, S. Silvestri, K. A. Nelson, E. Riedle, and R. W. Schoenlein, Springer Series in Chemical Physics, Vol. 92 (Springer-Verlag, New York, 2009), pp. 651–653.
[41] D. Turchinovich, J. M. Hvam, and M. C. Hoffmann, Phys. Rev. B **85**, 201304 (2012).
[42] L. Palfalvi, J. Hebling, J. Kuhl, A. Peter, and K. Polgar, J. Appl. Phys. **97**, 123505 (2005).
[43] J. D. Jackson, *Classical Electrodynamics* (Wiley, New York, 1998).
[44] G. A. Korn and T. M. Korn, *Mathematical Handbook for Scientists and Engineers*, 2nd ed. (McGraw-Hill, New York, 1968).
[45] S. J. Farlow, *Partial Differential Equations for Scientists and Engineers* (Dover, New York, 1993).
[46] V. G. Bespalov, V. N. Krylov, S. E. Putilin, and D. I. Stasel'ko, Opt. Spectrosc. **93**, 148 (2002).
[47] V. G. Bespalov, S. A. Kozlov, Y. A. Shpolyanskii, and A. N. Sutyagin, J. Opt. Technol. **65**, 823 (1998).